HOKKAIDO UNIVERSITY

Title	Surface mass balance of the Greenland ice sheet in the regional climate model HIRHAM5: Present state and future prospects
Author(s)	Mottram, Ruth; Boberg, Fredrik; Langen, Peter; Yang, Shuting; Rodehacke, Christian; Christensen, Jens Hesselbjerg; Madsen, Marianne Sloth
Citation	低温科学, 75, 105-115
Issue Date	2017-03-31
DOI	10.14943/lowtemsci.75.105
Doc URL	http://hdl.handle.net/2115/65106
Type	bulletin (article)
File Information	12_105-115.pdf

Instructions for use

Hokkaido University Collection of Scholarly and Academic Papers : HUSCAP

低温科学 75 （2017） 105-115
doi: 10.14943/lowtemsci. 75. 105

Surface mass balance of the Greenland ice sheet in the regional climate model HIRHAM5: Present state and future prospects

Ruth Mottram[1]*, Fredrik Boberg[1], Peter Langen[1], Shuting Yang[1], Christian Rodehacke[1], Jens Hesselbjerg Christensen[1], Marianne Sloth Madsen[1]

Received 1 February 2017, accepted 9 February 2017

Surface mass balance (SMB) is the builder of the Greenland ice sheet and the driver of ice dynamics. Quantifying the past, present and future state of SMB is important to understand the drivers and climatic processes that control SMB, and to both initialize and run ice sheet models which will help clarify sea level rise, and how likely changes in ice sheet extent feedback within the climate system.

Regional climate models (RCMs) and climate reanalysis are used to quantify SMB estimates. Although different models have different spatial and temporal biases and may include different processes giving significant uncertainty in both SMB and the ice sheet dynamic response to it, all RCMs show a recent declining trend in SMB from the Greenland ice sheet, driven primarily by enhanced melt rates. Here, we present new simulations of the Greenland ice sheet SMB at 5 km resolution from the RCM HIRHAM5. The RCM is driven by the ERA-Interim reanalysis and the global climate model (GCM) EC-Earth v2.3 to make future projections for climate scenarios RCP8.5 and RCP4.5.

Future estimates of SMB are affected by biases in driving global climate models, and feedbacks between the ice sheet surface and the global and regional climate system are neglected, likely resulting in significant underestimates of melt and precipitation over the ice sheet. These challenges will need to be met to better estimate the role climate change will have in modulating the surface mass balance of the Greenland ice sheet.

Keywords: Greenland ice sheet, surface mass balance, climate, climate modelling, ice sheet modelling

1. Introduction

The Greenland ice sheet is famously the second largest land ice mass on the planet, containing around 2.85 million km^3 of ice over an area of 1.71 million km^2, equivalent to 7.2 m sea level rise (IPCC, 2013). Results from remote sensing missions such as the GRACE gravimetry satellites indicate a recent significant negative mass budget, with around −234±20 Gt of net mass (Barletta et al., 2013) being lost each year including both the contribution from precipitation and surface mass balance and the dynamic contribution of calving from icebergs and submarine melt (Shepherd et al., 2012). The surface mass balance component is by far the most important component of the mass budget since it includes both positive (accumulation by precipitation) and negative (melt and runoff) terms, though around one third to one half of the mass lost by the ice sheet is from calving glaciers (Enderlin et al., 2014).

*Corresponding author
e-mail：rum@dmi.dk
1）Danish Meteorological Institute, Copenhagen, Denmark

Table 1：Comparison of surface mass balance components calculated for the present day using different models. Note that, as Vernon et al. (2013) point out, these models also have different resolutions and different ice masks, so that the numbers are not quite comparable. Therefore, we include in the right most column values from that study that compare the RACMO and MAR models using the same ice mask and forcing data, though with differing model resolution.

Model	Mean annual surface mass balance (Gt year^{-1})	Mean annual precipitation (Gt year^{-1})	Mean annual runoff (Gt year^{-1})	Mean annual surface mass balance (Gt year^{-1}) 1960–2008, from Vernon et al. (2013)
HIRHAM5 (1980–2014) (this study)	360 ± 134	866 ± 70	446 ± 109	—
RACMO (1991–2015) (van den Broeke et al., 2016)	306 ± 120	712 ± 70	363 ± 102	470
MAR (1980–2015) (Fettweis et al., 2016)	480 ± 87	711 ± 61	220 ± 52	432

SMB is not only important in itself, but is also important for ice sheet modelling studies where SMB, or the degree day approximation of it based on temperature and precipitation, is used to drive ice sheet dynamics. We thus use high-resolution regional climate models to clarify both the current state of the ice sheet surface mass balance and its future prospects under climate change scenarios with the aim of also providing SMB forcing for dynamical ice sheet models.

Previous work on Greenland ice sheet mass balance has used the regional climate models MAR and RACMO as well as HIRHAM5 to determine the present-day and future surface mass balance (Lucas-Picher et al., 2012; Rae et al., 2012; Langen et al., 2015). Other models, such as SnowModel (Mernild et al., 2009) or Hanna et al.'s (2013) dECMWF model are not strictly regional climate models, but use either model output to drive a separate snow scheme (SnowModel) or use statistical methods to downscale output that is then used to calculate SMB based on temperature index methods (dECMWF) (Church et al., 2013).

These models have previously estimated the mean annual SMB to be in the range 340 to 470 Gt per year (see Table 1), though note that both forcing data, time period, resolution as well as processes and ice mask all vary in these estimates, and this can have a significant effect on any one models SMB estimate when compared to the others, as shown by Vernon et al. (2013). An earlier version of HIRHAM5 showed an average annual SMB of 188 Gt year^{-1} over the whole ice sheet for the period 1990 to 2008 (Rae et al., 2012). However, this version was run at a coarser resolution of 25 km and with a significantly simplified snow model to calculate surface mass balance. Our current version of HIRHAM5 is run at 5 km resolution and was used by Langen et al. (2015) to show regional changes in Greenland. Here we use a further updated version of the model (Langen et al., 2017) to calculate SMB across the Greenland ice sheet and to make future projections when forced with a global climate model.

The high resolution of the HIRHAM5 model in this set of simulations means that we can assess the performance of the model on both the narrow ablation zone and on small outlet glaciers and peripheral ice caps without needing to statistically account for elevation changes, as performed for example by Noël et al. (2016). Results by Langen et al. (2017) show that the model performs well in these marginal areas, even without elevation correction, when compared with ablation and weather station measurements predominantly in the ablation zone compiled by Machguth et al. (2016). Similarly, analysis by Schmidt et al. (submitted) shows that the model works very well over the small Icelandic ice cap Vatnajökull, which is analogous to peripheral glaciers in Greenland. At the present day up to 10% of the mass loss from Greenland is currently contributed by these small glaciers and ice caps (Bolch et al., 2013) and it is therefore important to be able to account for their surface mass balance correctly in model projections.

In this study we use a separate dataset of shallow firn cores from around the accumulation zone in Greenland compiled by Buchardt et al. (2012) to evaluate how the model performs at higher elevations. In the future, dynamically driven changes in ice sheet altitude, due to increasing melt rates and projected increases in precipitation, will likely have important feedbacks on both orographic precipitation and melt rates. In this sense the use of high-resolution simulations offers additional value in both identifying and quantifying feedbacks between ice and atmosphere.

The combination of surface mass balance modelling with estimates of total mass budget derived from both altimetry and flux gate calculations (Rignot et al., 2011) and the satellite gravimetry mission GRACE offers the possibility of estimating the relative importance of surface mass processes and calving dynamics (Shepherd et al., 2012). In this paper we focus on the surface mass budget contribution both at the present day and in the future.

2. Regional climate model HIRHAM5

In this study we use the latest version of the RCM HIRHAM5 (Langen et al., 2017) for a domain covering Greenland, Iceland and parts of Arctic Canada (Figure 1). The RCM was developed at the Danish Meteorological Institute (DMI) (Christensen et al., 2006) from the HIRLAM7 numerical weather prediction model (Eerola, 2006) and the ECHAM5 global climate model (Roeckner et al., 2003). The model is very similar in set-up to that fully described in Langen et al. (2015, 2017) and Lucas-Picher et al. (2014) run on a $0.05° \times 0.05°$ rotated polar grid for a 35 year period (1980–2014). For the present-day simulations HIRHAM5 was forced on the lateral boundaries by the ERA-Interim reanalysis product (Dee et al., 2011) every 6 hours. On the lower boundary, sea surface temperatures (SSTs) and sea ice concentration were statistically interpolated from the ERA-Interim data format to the model resolution and prescribed daily. The model runs freely within the boundaries and only temperature, pressure, relative humidity and wind velocities are used in lateral boundary forcing. The current set-up of HIRHAM5 has 31 vertical levels in the atmosphere, 5 vertical levels in the soil, including glaciers and snow and a 90 second dynamical time step. A

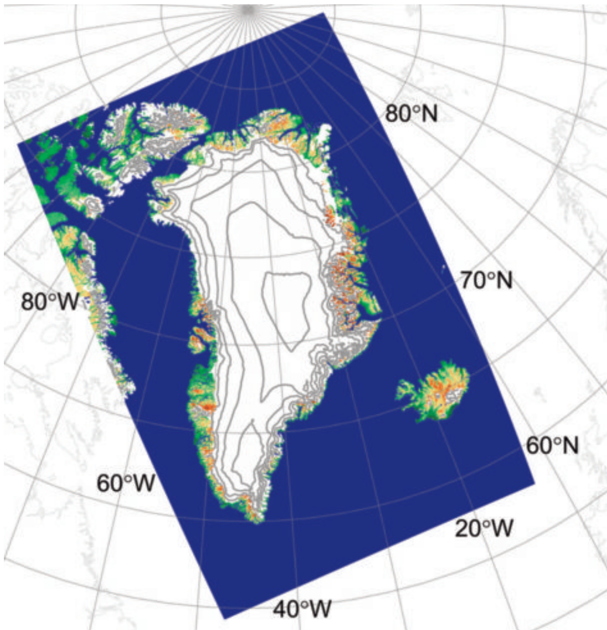

Figure 1 : The domain, topography and ice mask used in all HIRHAM5 simulations for Greenland.

32 layer snow pack model is applied offline over glacier points to calculate surface mass balance using more detailed snowpack processes (Langen et al., 2017; see below). The topography of Greenland is taken from Bamber et al. (2001), and it should be noted that although snow is allowed to accumulate without limits over glaciers and ice sheets, the elevation of the ice sheet surface remains fixed during the simulation such that there are no feedbacks between surface mass balance and ice dynamics. The ice mask used in this simulation is updated from that used by Langen et al. (2015) to that produced by Citterio and Ahlstrøm (2013) with additional data for Iceland provided by the Icelandic Met Office (Figure 1).

Using this same set-up we also forced HIRHAM5 on the lateral boundaries with fields from the EC-Earth v2.3 GCM (Hazeleger et al., 2012) in order to produce future climate simulations of the surface mass balance of Greenland. In this set-up, EC-Earth was run at a resolution of 125 km using the historical emissions and RCP4.5 and 8.5 climate scenarios in the CMIP5 set-up (Taylor et al., 2012). Both the lateral boundaries and the ocean SSTs and sea ice were provided by the driving GCM to the HIRHAM5 model for downscaling experiments. The future projections were run as transient 20 year time slices for the mid and end of the 21st century using RCP4.5 and RCP8.5 scenarios, as well as a simulation using historical emissions for the period 1991–2010, used as a control run to assess performance of the EC-Earth model at the present day.

Prior to running the simulations, the inclusion of the full snowpack model as detailed below meant that an adequate spin-up was required in particular for the snow and ice properties to reach equilibrium with the climate. For this purpose we ran the HIRHAM5 model for one year, and then used the atmospheric output to run the surface scheme offline repeatedly until decadal means of runoff and subsurface temperatures ceased to show transient variability (in this case, after 70 years of simulation time).

The full details of the surface mass balance calculation in HIRHAM5 are given in Langen et al. (2017), but a quick summary is given here to assist in interpreting results. Surface mass balance is calculated from the sum of the precipitation and the runoff (a negative term). Runoff is calculated from the melt of surface snow and ice, accounting for the effects of retention and refreezing within any snowpack that overlies the glacier ice. Rain on snow is similarly accounted for, though rain on bare ice is assumed to runoff directly. There is currently no runoff routing scheme from the model and therefore no superimposed ice formation on bare glacier ice. However, with the introduction of a sophisticated firn model, processes now include densification, snow grain growth, snow state-dependent hydraulic conductivity, superimposed ice formation at the base of the snow pack on glacier ice, and irreducible water saturation. The accommodation for water retention in excess of the irreducible saturation means that formation of both perennial firn aquifers and perched ice lenses occurs within the snowpack (Langen et al., 2017).

The HIRHAM5 surface scheme uses a standard energy balance scheme to calculate the melt of snow and underlying glacier ice:

$$Q_m = S_{in}(1-\alpha) + L_{in} - L_{out} + Q_H + Q_L$$

$$M = \frac{Q_m}{\rho_w L_f} \tag{1}$$

where Q_m is the total energy flux at the surface, S_{in} is the incoming shortwave radiation, α is the surface albedo, L_{in} and L_{out} are the incoming and outgoing longwave radiative fluxes, respectively, and Q_H and Q_L are the sensible and latent heat fluxes. As the skin temperature cannot rise above the freezing point of 273.15° K on a glacier surface, the excess energy is instantaneously used for melt, M, accounting for the density of water, ρ_w, and the release of latent heat, L_f.

Meltwater and rain that falls over glaciers are grouped together in the model as the liquid water fraction. Where there is a snow layer overlying the glacier surface, the liquid water percolates into the deeper layers according to a given threshold of irreducible water saturation and, if there is a sufficient cold content, refreezes within the snowpack. In the sub-surface scheme over glaciers, there are 32 layers of unequal thickness of snow or ice or some combination of the two depending on the depth of surface snow. The thickness of the layers in the subsurface scheme over glaciers or snow-covered land is calculated in metres of water equivalent to allow for the easy calculation of mass change, with different heat diffusion and conductivity parameter values used for water, ice and snow within the snowpack. As surface melting and rainfall occur, the water percolates into the lower layers and retention is calculated by allowing liquid water in excess of the density-dependent irreducible water saturation within the layer to percolate to the layer below. Ice is formed in the snowpack layers based on the "cold content" in each layer. The cold content determines how much liquid water can freeze within that layer based on the energy required to heat the snow and ice mass to the freezing point in each layer. This is used to instantaneously freeze as much liquid water as is available or as the cold content allows, within a single time step. This mass is then transferred to the ice fraction and the temperature of the layer is calculated taking into account the latent heat release to conserve energy.

As the subsurface scheme extends to a depth of 60 metres water equivalent (mwe), if there is less than 60 mwe snow on the glacier surface then the layers of the subsurface scheme have the properties of ice. No percolation of meltwater is allowed through ice layers, but energy fluxes are diffused through all the layers. We assume that the ice layers from the glacier coming into the column at the base of the subsurface scheme have a temperature equivalent to the annual mean

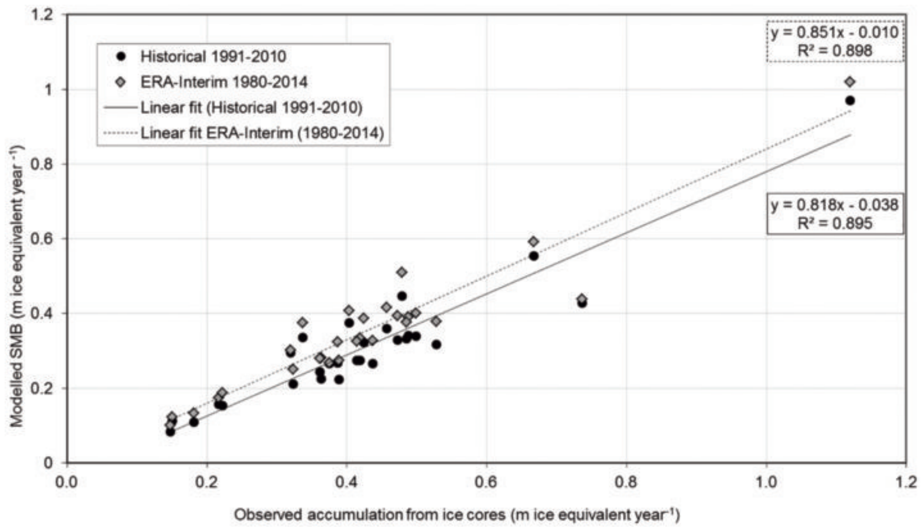

Figure 2 : Comparison of observed SMB from shallow core data compiled by Buchardt et al. (2012) with modelled values from the ERA-Interim forced simulation and the historical emissions scenario of EC-Earth.

temperature of that grid square location.

As Langen et al. (2017) discuss, the albedo of the model is one of the largest sources of uncertainty in the mass balance estimate. In the simulations we present here, we use the internally derived albedo scheme, rather than an externally forced albedo product based on MODIS as also described in Langen et al. (2017). This allows us to make a direct comparison of the present-day SMB with the future projections where data such as MODIS is of course unavailable. The albedo scheme in the model has a cold (< -5°C) snow albedo of 0.85, linearly decreasing to 0.65 as temperature increases from -5°C to 0°C. The albedo for bare ice is fixed at 0.4 with a linear function for thin (<3 cm) snow between the two values. Broadband values lower than 0.4 do occur as shown in measurements at the PROMICE automatic weather stations (van As et al., 2016) and MODIS data products (Stroeve et al., 2006). Similarly, freshly exposed ice can have much brighter values for surface albedo, but the values in the current scheme were optimized over the ice sheet by Nielsen-Englyst (2015). Langen et al. (2017) show that significant biases still persist in albedo values over the ice sheet; however, partly due to processes such as dust accumulation and biological activity that are not currently included. Recent work by Stibal et al. (2015) demonstrates the importance of microorganisms and melted out dust on the Greenland ice sheet, and the development of appropriate parameterizations is an area of active research.

The HIRHAM5 model performance is comprehensively evaluated in Langen et al. (2015, 2017) using weather station data, shallow firn cores and historical SMB observations from Machguth et al. (2016). Their results show that the model performs extremely well over Greenland, reproducing air temperatures and accumulation rates well on average. However, some biases in radiation suggest that cloud cover or cloud optical thickness may not be fully captured in the model. Similarly, HIRHAM5 is not able to capture deep cold inversion layers over the ice sheet, and evidence from Fausto et al. (2016) suggests that during extreme melt events, such as were observed in 2012, the model underestimated the sensible heat flux by up to 75% in some locations.

Analysis of the same ERA-Interim simulation by Schmidt et al. (submitted) over Icelandic glaciers shows that HIRHAM5 also performs well over small glaciers and ice caps, particularly with regard to accumulation rates. However, Schmidt et al. (submitted) also identify that orographically forced precipitation is overestimated on the upslope with a possible small dry bias downwind. This is a common problem in hydrostatic models where the dynamical scheme means that precipitation is handled diagnostically (Forbes et al., 2011).

3. Results and discussion

3.1 Surface mass balance

In Figure 2 we complement the model analysis of Langen et al. (2017) by comparing observed surface mass balance from stake measurements and shallow firn cores (Buchardt et al., 2012) with those calculated from the same grid cell in HIRHAM5. Figure 2 shows that the model is able to reproduce the pattern of SMB over the ice sheet when forced with both ERA-Interim ($R^2 = 0.898$) and EC-Earth ($R^2 = 0.895$), though with a very slightly more pronounced dry bias in the historical simulation. For this comparison we took the decadal mean SMB from firn cores that cover all or part of the period of the ERA-Interim driven simulation. Although the model reproduces the observed SMB pretty well, it is important to note that observed SMB rates are determined by short- and medium-term climate variability that may not be captured by climate models, thus leading to the poorer fit against these point measurements. This point is underlined in Table 2 where there are large differences in SMB calculated on a decadal timescale and compared across the full 1980–2014 simulation period. However, note that in Table 1 the total SMB for Greenland is close to, but not exactly the same as comparable simulations using other RCMs.

As we plot both model simulations against the same core data for comparison, it is interesting to see that the pattern of high and low accumulation rates across Greenland are reflected in both simulations (see also Figure 5), but the magnitude differs slightly with the EC-Earth historical run having a generally lower value. This suggests that in the accumulation zone at least, both models have a dry bias, though that in the EC-Earth simulation is somewhat stronger. Observational data from the south-east of Greenland, the region with highest precipitation, are too sparse to assess how well the model reproduces it. For the only core data we have from south-east Greenland, the model under-estimates SMB in both simulations, though to a lesser extent in the ERA-Interim simulation. More observations in this region would be helpful in both evaluating the model and comparing results from this simulation with other models.

Table 2 : SMB calculated using the ERA-Interim driven simulation in different decades and overall. The choice of period can make a large difference in the estimated annual mean SMB.

Period	Mean annual SMB (Gt year^{-1})
1980–2014	360 ± 134
1980–1990	375 ± 130
1991–2010	346 ± 132
2000–2014	277 ± 101

3.2 Surface mass balance components

Figure 3 shows the surface mass balance of Greenland as a whole for the period 1980 to 2014. There

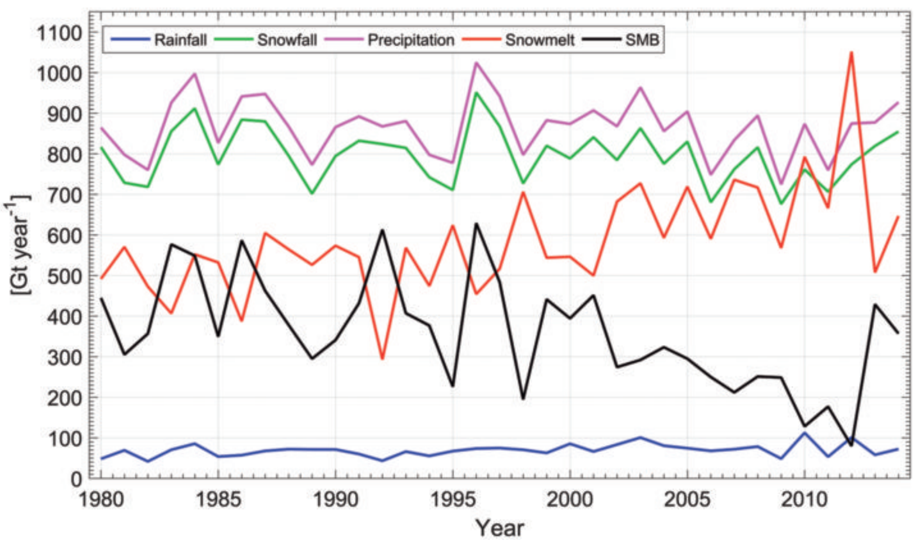

Figure 3 : Annual mean components of surface mass balance for the present day in the ERA-Interim simulation.

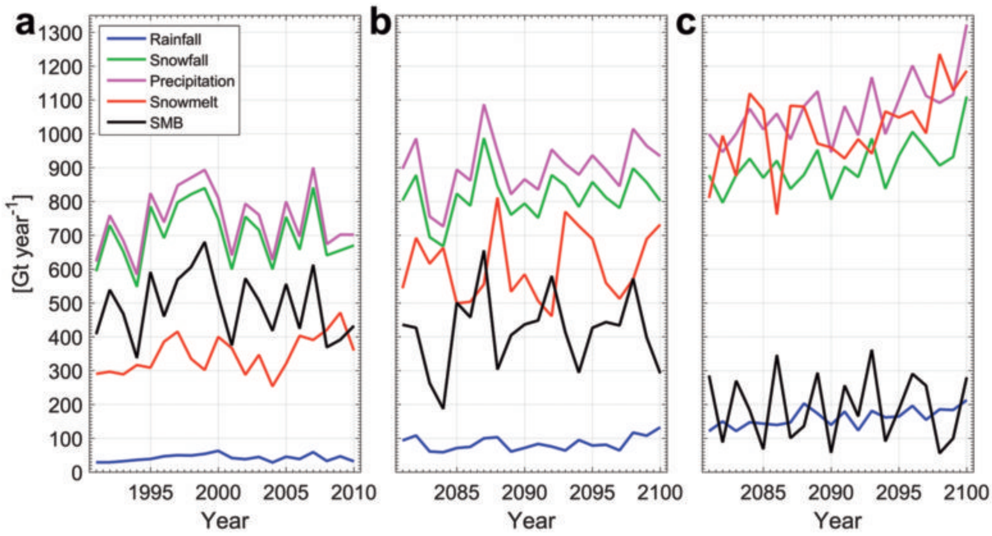

Figure 4 : Annual mean components of surface mass balance for a) the historical emissions simulation, and the end of the century under b) RCP4.5 and c) RCP8.5 scenarios.

is a strong declining trend in SMB in the most recent decade driven largely by increased melt and runoff rates. The interannual variability is however also large and shows the importance of long time series in analyzing the SMB trends. There has also been an increase in rainfall events over Greenland, though this is barely discernable over the whole ice sheet. However, work by Doyle et al. (2015), analyzing the ERA-Interim simulation, shows that in western Greenland, rainfall events occurring more frequently at higher altitudes over the ice sheet have a distinct impact on the dynamics of the ice sheet.

Comparison between Figures 3 and 4a shows that the EC-Earth historical simulation underestimates snowfall across the whole ice sheet compared to ERA-Interim; however, melt rates are also lower and these two components compensate for each other to some extent when estimating total SMB. Note that the firn core observations in Figure 2 are confined to the higher accumulation zone where differences in melt and runoff rates between the two historical period simulations are minor.

Figures 4b and 4c show the end of the 21st century under two different climate scenarios. A comparison between Figures 3 and 4b show that under the RCP4.5 scenario, the model expects a similar, though still higher mean annual SMB to that of the last decade in ERA-Interim, with both higher precipitation and higher melt rates than the historical simulation. It is important to note that in Figure 5 both the pattern of precipitation and melt appear comparable with that given by the ERA-interim simulation, suggesting that EC-Earth does not simulate significant changes in circulation.

There is a documented bias in EC-Earth v2.3, which is colder in the Arctic region during the historical period than observations suggest (Hazeleger et al., 2012). This is partly attributable to a larger area covered by sea ice than observed and possibly also to the albedo scheme in Greenland (Helsen et al., 2016) in the standard EC-Earth set-up. Ongoing work to couple EC-Earth to an ice sheet model (Madsen et al., in preparation) may improve this in the future.

On the other hand, the sources of high melt rates observed over the ice sheet in recent years appear to be persistent blocking high pressure systems that may simply reflect internal variability within the climate system (Fettweis et al., 2013). Although recent work by Hanna et al. (2016) suggests that some of the recent increases in persistent anomalies could be a climate change signal, analysis of data from a wide range of climate models within the CMIP5 archive does not seem to indicate this is an expected signal of climate change. The higher SMB in the EC-Earth simulations suggests that the cold bias in EC-Earth observed historically in the Arctic persists through the 21st century. Assuming that the ERA-Interim driven SMB is accurate, it suggests that the EC-Earth climate simulations may be under-estimating the rate of climate change in the Arctic over this century. However, the much lower SMB in

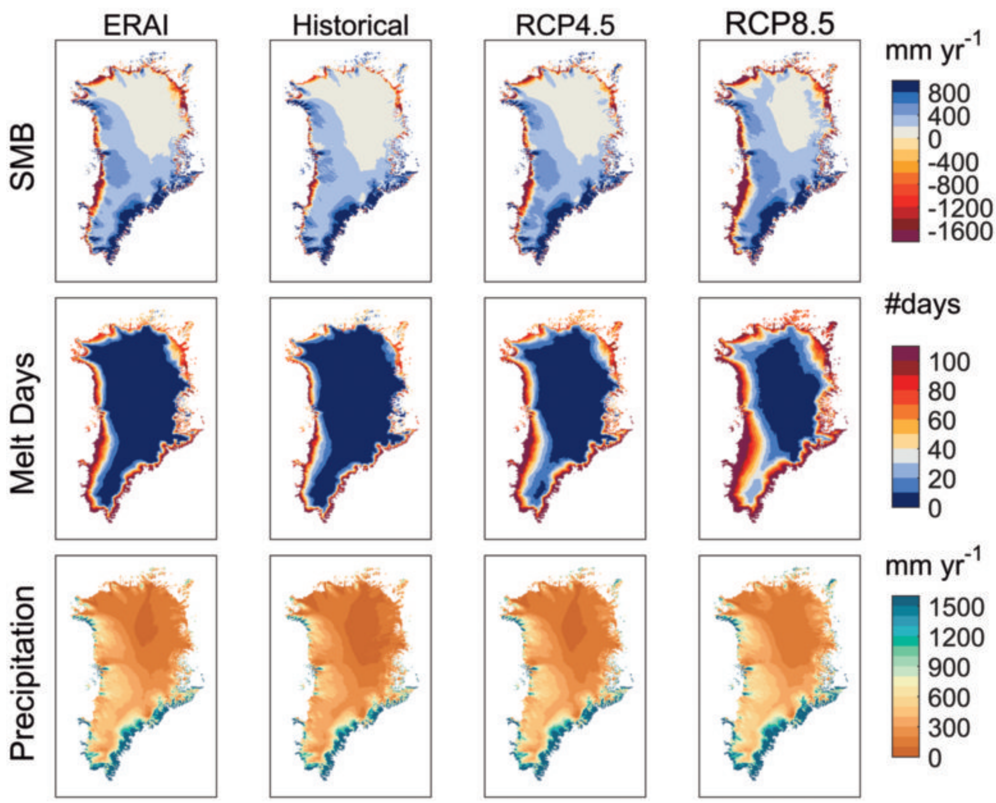

Figure 5：SMB, precipitation and the number of melt days for the ERA-Interim and historical emissions scenario as well as the end of the 21st century RCP4.5 and RCP8.5 scenarios.

the RCP8.5 simulation at the end of the 21st century reflects a much greater enhancement to Arctic warming in the higher RCP8.5 emissions scenario.

The change in ice sheet SMB expected under climate scenarios RCP4.5 and RCP8.5 both show increased precipitation and a significant increase in melt compared in melt rates compared to the historical simulation. These increases are scaled by scenario so that RCP4.5 has a lower increase in melt than RCP8.5.

Table 3 summarizes the projected change in SMB for the mid-century and end of the century simulations for the two different climate scenarios. The plots in Figure 5 show that, while the precipitation pattern remains similar through the projections, the melt area will expand, particularly in western and northern Greenland and over the saddle region in the south, with the magnitude of this expansion determined by the scenario. The increase in precipitation projected by the model is largely confined to the south-east, with a very small increase in northern Greenland, this represents an intensification of existing precipitation patterns.

One potential source of uncertainty in this study is the fixed ice sheet mask during the simulations.

Table 3：SMB from historical, mid-century and end of the century simulations for two different climate scenarios, RCP4.5 and RCP8.5 dynamically downscaled from EC-Earth using the HIRHAM5 set-up. Note that the historical emissions scenario is used for the period 1990-2006 and RCP4.5 for the remaining four years.

	Mean annual surface mass balance (Gt year^{-1})		
Simulation period	Historical	RCP4.5	RCP8.5
1991-2010	492±94	—	—
2031-2050	—	460±79	414±65
2081-2100	—	418±109	193±99

Neither the ablation — elevation feedback, which leads to lowering of the ice sheet margin and thus increased ablation rates, nor the potential migration of orographic precipitation as the ice sheet margin retreats are included. Similarly, with high ablation rates, the lower ablation zone and peripheral glaciers will be lost at some point, but these are still in the ice mask at the end of century when SMB is calculated in these simulations. This suggests that the very low annual SMB under RCP8.5 may be an understimate. Further analysis of the difference between ice sheet and peripheral glaciers is required to account for this. A dynamical ice sheet model run coupled with the climate model is also required to answer these questions fully, and sensitivity experiments planned for future work will also help to determine whether these effects are important.

4. Conclusions

In this paper we present a summary of the present-day surface mass balance in Greenland. Our results and those reported in Langen et al. (2017) show that the ice sheet and peripheral glaciers are well represented at the present day, but biases from global climate model forcing underestimate the amount of melt and precipitation currently in Greenland compared to reanalysis driven simulations.

In the future, downscaling global climate model simulations suggest that an increase in melt and runoff, only partially balanced by a small increase in precipitation, is likely to lead to increasing mass loss from the ice sheet, with the total magnitude determined by the forcing due to greenhouse gas emissions.

The small size of peripheral glaciers means that many of them may disappear entirely in this century. However, the fixed ice mask in this simulation means that neither the changing distribution of ice nor elevation-related feedbacks such as ablation area increase due to declining elevation, nor precipitation migration due to changes in orography, are considered here. These are areas for future study.

Data availability

HIRHAM5 simulation output is freely available at http: //prudence. dmi. dk/data/temp/RUM/HIRHAM/GL2 (or contact the authors directly).

Acknowledgements

Research reported in this paper was supported in part by the ERC Synergy project ice2ice (ERC grant 610055) from the European Community's Seventh Framework Programme (FP7/2007-2013) and the RETAIN project, funded by the Danish Council for Independent research (Grant no. 4002-00234). Ruth Mottram gratefully acknowledges the invitation to the international workshop "Greenland ice sheet mass loss and its impact on global climate change" under the SIGMA (Snow Impurity and Glacial Microbe effects on abrupt warming in the Arctic) project, the ArCS (Arctic Challenge for Sustainability) Project and the Joint Research Program of the Institute of Low Temperature Science, Hokkaido University. We thank Ralf Greve for a thorough review which substantially improved the paper.

References

Bamber, J. L., R. L. Layberry, and S. P. Gogineni (2001) A new ice thickness and bed data set for the Greenland ice sheet: 1. Measurement, data reduction, and errors. *J. Geophys. Res. Atmos.*, **106**, 33773-33780, doi: 10.1029/2001JD900054.

Barletta, V. R., L. S. Sørensen, and R. Forsberg (2013) Scatter of mass changes estimates at basin scale for Greenland and Antarctica. *Cryosphere*, **7**, 1411-1432, doi: 10.5194/tc-7-1411-2013.

Bolch, T., L. Sandberg Sørensen, S. B. Simonsen, N. Mölg, H. Machguth, P. Rastner, and F. Paul (2013) Mass loss of Greenland's glaciers and ice caps 2003-2008 revealed from ICESat laser altimetry data. *Geophys. Res. Lett.*, **40**, 875-881, doi: 10.1002/grl.50270.

Buchardt, S. L., H. B. Clausen, B. M. Vinther, and D. Dahl-Jensen (2012) Investigating the past and recent δ^{18}O-accumulation relationship seen in Greenland ice cores. *Clim. Past*, **8**, 2053-2059, doi: 10.5194/cp-8-2053-2012.

Christensen, O. B., M. Drews, J. H. Christensen, K. Dethloff, K. Ketelsen, I. Hebestadt, and A. Rinke (2006) The HIRHAM regional climate model version 5. DMI Technical Report 06-17, URL: https: //www. dmi. dk/fileadmin/Rapporter/TR/tr06-17.pdf.

Church, J. A., P. U. Clark, A. Cazenave, J. M. Gregory, S. Jevrejeva, A. Levermann, M. A. Merrifield, G. A. Milne, R. S. Nerem, P. D. Nunn, A. J. Payne, W. T. Pfeffer, D. Stammer, and A. S. Unnikrishnan (2013) Sea level change. In: T. F. Stocker, D. Qin, G.-K. Plattner, M. Tignor, S. K. Allen, J. Boschung, A. Nauels, Y. Xia, V. Bex, and P. M. Midgley (Eds.), *Climate Change 2013: The Physical Science Basis. Contribution of Working Group I to the Fifth Assessment Report of the Intergovernmental Panel on Climate Change.* Cambridge University Press, Cambridge, United Kingdom and New York, NY, USA, pp.1137-1216.

Citterio, M., and A. P. Ahlstrøm (2013) Brief communication "The aerophotogrammetric map of Greenland ice masses". *Cryosphere*, **7**, 445-449, doi: 10.5194/tc-7-445-2013.

Dee, D. P., S. M. Uppala, A. J. Simmons, P. Berrisford, P. Poli, S.

Kobayashi, U. Andrae, M. A. Balmaseda, G. Balsamo, P. Bauer, P. Bechtold, A. C. M. Beljaars, L. van de Berg, J. Bidlot, N. Bormann, C. Delsol, R. Dragani, M. Fuentes, A. J. Geer, L. Haimberger, S. B. Healy, H. Hersbach, E. V. Hólm, L. Isaksen, P. Kållberg, M. Köhler, M. Matricardi, A. P. McNally, B. M. Monge-Sanz, J.-J. Morcrette, B.-K. Park, C. Peubey, P. de Rosnay, C. Tavolato, J.-N. Thépaut, and F. Vitart (2011) The ERA-Interim reanalysis: configuration and performance of the data assimilation system. *Q. J. R. Meteorol. Soc.*, **137**, 553–597, doi: 10.1002/qj.828.

Doyle, S. H., A. Hubbard, R. S. W. van de Wal, J. E. Box, D. van As, K. Scharrer, T. W. Meierbachtol, P. C. J. P. Smeets, J. T. Harper, E. Johansson, R. H. Mottram, A. B. Mikkelsen, F. Wilhelms, H. Patton, P. Christoffersen, and B. Hubbard (2015) Amplified melt and flow of the Greenland ice sheet driven by late-summer cyclonic rainfall. *Nat. Geosci.*, **8**, 647–653, doi: 10.1038/ngeo2482.

Eerola, K. (2006) About the performance of HIRLAM version 7.0. *HIRLAM Newsl.*, **51**, 93–102.

Fausto, R. S., D. van As, J. E. Box, W. Colgan, P. L. Langen, and R. H. Mottram (2016) The implication of nonradiative energy fluxes dominating Greenland ice sheet exceptional ablation area surface melt in 2012. *Geophys. Res. Lett.*, **43**, 2649–2658, doi: 10.1002/2016GL067720.

Fettweis, X., E. Hanna, C. Lang, A. Belleflamme, M. Erpicum, and H. Gallée (2013) Important role of the mid-tropospheric atmospheric circulation in the recent surface melt increase over the Greenland ice sheet. *Cryosphere*, **7**, 241–248.

Forbes, R., A. M. Tompkins, and A. Ungatch (2011) A new prognostic bulk microphysics scheme for the IFS. Technical Memorandum No.649, ECMWF.

Hanna, E., T. Cropper, R. Hall, and J. Cappelen (2016) Greenland Blocking Index 1851–2015: a regional climate change signal. *Int. J. Climatol.*, **36**, 4847–4861, doi: 10.1002/joc.4673.

Hanna, E., F. J. Navarro, F. Pattyn, C. M. Domingues, X. Fettweis, E. R. Ivins, R. J. Nicholls, C. Ritz, B. Smith, S. Tulaczyk, P. L. Whitehouse, and H. J. Zwally (2013) Ice-sheet mass balance and climate change. *Nature*, **498**, 51–59.

Hazeleger, W., X. Wang, C. Severijns, S. Ştefănescu, R. Bintanja, A. Sterl, K. Wyser, T. Semmler, S. Yang, B. van den Hurk, T. van Noije, E. van der Linden, and K. van der Wiel (2012) EC-Earth V2.2: description and validation of a new seamless earth system prediction model. *Clim. Dyn.*, **39**, 2611–2629, doi: 10.1007/s00382-011-1228-5.

IPCC (2013) *Climate Change 2013: The Physical Science Basis. Contribution of Working Group I to the Fifth Assessment Report of the Intergovernmental Panel on Climate Change* (Eds. T. F. Stocker, D. Qin, G.-K. Plattner, M. Tignor, S. K. Allen, J. Boschung, A. Nauels, Y. Xia, V. Bex, and P. M. Midgley). Cambridge University Press, Cambridge, United Kingdom and New York, NY, USA.

Langen, P. L., R. H. Mottram, J. H. Christensen, F. Boberg, C. B. Rodehacke, M. Stendel, D. van As, A. P. Ahlstrøm, J. Mortensen, S. Rysgaard, D. Petersen, K. H. Svendsen, G. Aðalgeirsdóttir, and J. Cappelen (2015) Quantifying energy and mass fluxes controlling Godthåbsfjord freshwater input in a 5 km simulation (1991–2012). *J. Climate*, **28**, 3694–3713, doi: 10.1175/JCLI-D-14-00271.1.

Langen, P. L., R. S. Fausto, B. Vandecrux, R. H. Mottram, and J. E. Box (2017) Liquid water flow and retention on the Greenland ice sheet in the regional climate model HIRHAM5: Local and large-scale impacts. *Front. Earth Sci.*, **4**, 110, doi: 10.3389/feart.2016.00110.

Lucas-Picher, P., M. Wulff-Nielsen, J. H. Christensen, G. Aðalgeirsdottir, R. Mottram, and S. B. Simonsen (2012) Very high resolution regional climate model simulations over Greenland: Identifying added value. *J. Geophys. Res. Atmos.*, **117**, D02108, doi: 10.1029/2011JD016267.

Machguth, H., H. H. Thomsen, A. Weidick, A. P. Ahlstrøm, J. Abermann, M. L. Andersen, S. B. Andersen, A. A. Bjørk, J. E. Box, R. J. Braithwaite, C. E. Bøggild, M. Citterio, P. Clement, W. Colgan, R. S. Fausto, K. Gleie, S. Gubler, B. Hasholt, B. Hynek, N. T. Knudsen, S. H. Larsen, S. H. Mernild, J. Oerlemans, H. Oerter, O. B. Olesen, C. J. P. P. Smeets, K. Steffen, M. Stober, S. Sugiyama, D. van As, M. R. van den Broeke, and R. S. W. van de Wal (2016) Greenland surface mass-balance observations from the ice-sheet ablation area and local glaciers. *J. Glaciol.*, **62**, 861–887, doi: 10.1017/jog.2016.75.

Mernild, S. H., G. E. Liston, C. A. Hiemstra, K. Steffen, E. Hanna, and J. H. Christensen (2009) Greenland Ice Sheet surface mass-balance modelling and freshwater flux for 2007, and in a 1995–2007 perspective. *Hydrol. Process.*, **23**, 2470–2484, doi: 10.1002/hyp.7354.

Noël, B., W. J. van de Berg, H. Machguth, S. Lhermitte, I. Howat, X. Fettweis, and M. R. van den Broeke (2016) A daily, 1 km resolution data set of downscaled Greenland ice sheet surface mass balance (1958–2015). *Cryosphere*, **10**, 2361–2377, doi: 10.5194/tc-10-2361-2016.

Nielsen-Englyst, P. (2015) *Impact of Albedo Parametrizations on Surface Mass Balance Runoff on the Greenland Ice Sheet.* Master Thesis, University of Copenhagen.

Rae, J. G. L., G. Aðalgeirsdottir, T. L. Edwards, X. Fettweis, J. M. Gregory, H. T. Hewitt, J. A. Lowe, P. Lucas-Picher, R. H. Mottram, A. J. Payne, J. K. Ridley, S. R. Shannon, W. J. van de Berg, R. S. W. van de Wal, and M. R. van den Broeke (2012) Greenland ice sheet surface mass balance: evaluating simulations and making projections with regional climate models. *Cryosphere*, **6**, 1275–1294, doi: 10.5194/tc-6-1275-2012.

Rignot, E., I. Velicogna, M. R. van den Broeke, A. Monaghan, and J. T. M. Lenaerts (2011) Acceleration of the contribution of the Greenland and Antarctic ice sheets to sea level rise. *Geophys. Res. Lett.*, **38**, L05503, doi: 10.1029/2011GL046583.

Roeckner, E., G. Bäuml, L. Bonaventura, R. Brokopf, M. Esch, M. Giorgetta, S. Hagemann, I. Kirchner, L. Kornblueh, E. Manzini, A. Rhodin, U. Schlese, U. Schulzweida, and A. Tompkins (2003) The atmospheric general circulation model ECHAM 5. Part I: Model description. Technical Report No.349, Max Planck Institute.

Schmidt, L. G. Aðalgeirsdóttir, S. Guðmundsson, P. L. Langen, F. Pálsson, R. Mottram, S. Gascoin, and H. Björnsson (submitted) Evaluating the surface energy balance in the HIRHAM5 regional climate model over Vatnajökull, Iceland, using automatic weather station data. *Cryosphere* (submitted MS No. tc-2017-14).

Shepherd, A., E. R. Ivins, G. A, V. R. Barletta, M. J. Bentley, S. Bettadpur, K. H. Briggs, D. H. Bromwich, R. Forsberg, N. Galin, M. Horwath, S. Jacobs, I. Joughin, M. A. King, J. T. M. Lenaerts, J. Li, S. R. M. Ligtenberg, A. Luckman, S. B. Luthcke, M. McMillan, R. Meister, G. Milne, J. Mouginot, A. Muir, J. P. Nicolas, J. Paden, A. J. Payne, H. Pritchard, E. Rignot, H. Rott, L. S. Sorensen, T. A. Scambos, B. Scheuchl, E. J. O. Schrama, B. Smith, A. V. Sundal, J. H. van Angelen, W. J. van de Berg, M. R. van den Broeke, D. G. Vaughan, I. Velicogna, J. Wahr, P. L. Whitehouse, D. J. Wingham, D. Yi, D. Young, and H. J. Zwally (2012) A reconciled estimate of ice-sheet mass balance. *Science*, **338**, 1183–1189, doi: 10.1126/science.1228102.

Stibal, M., E. Gözdereliler, K. A. Cameron, J. E. Box, I. T. Stevens, J. K. Gokul, M. Schostag, J. D. Zarsky, A. Edwards, T. D. L. Irvine-Fynn, and C. S. Jacobsen (2015) Microbial abundance in surface ice on the Greenland Ice Sheet. *Front. Microbiol.*, **6**, 225, doi: 10.3389/fmicb.2015.00225.

Van As, D., R. S. Fausto, J. Cappelen, R. S. W. van der Wal, R. J. Braithwaite, H. Machguth, C. Charalampidis, J. E. Box, A. M. Solgaard, A. P. Ahlstrøm, K. Haubner, M. Citterio, and S. B. Andersen (2016) Placing Greenland ice sheet ablation measurements in a multi-decadal context. *Geol. Surv. Den. Greenl. Bull.*, **35**, 71–74.

Vernon, C. L., J. L. Bamber, J. E. Box, M. R. van den Broeke, X. Fettweis, E. Hanna, and P. Huybrechts (2013) Surface mass balance model intercomparison for the Greenland ice sheet. *Cryosphere*, **7**, 599–614, doi: 10.5194/tc-7-599-2013.